

A EUROPEAN JOURNAL

CHEMPHYSICHEM

OF CHEMICAL PHYSICS AND PHYSICAL CHEMISTRY



Reprint

© Wiley-VCH Verlag GmbH & Co. KGaA, Weinheim

A Journal of



WILEY-VCH

www.chemphyschem.org

A Comparative Study on the Photophysics and Photochemistry of Xanthene Dyes in the Presence of Polyamidoamine (PAMAM) Dendrimers

Ernesto Maximiliano Arbeloa,* Carlos Mario Previtali, and Sonia Graciela Bertolotti^[a]

The photophysical and photochemical properties of the xanthene dyes Eosin Y, Erythrosin B, and Rose Bengal are evaluated in the presence of amino-terminated polyamidoamine (PAMAM) dendrimers of relatively high generation (G3–G5) in alkaline aqueous solution. UV/Vis absorption and fluorescence spectra of the dyes show bathochromic shifts, which correlate with the size of the dendrimer. Binding constants (K_{bind}) are calculated from absorption data. The resulting high K_{bind} values indicate strong interactions between both molecules. Triplet-

triplet absorption spectra of the dyes are recorded by laser flash photolysis, and a decrease in the triplet lifetimes is observed in the presence of dendrimers. At the same time, an increase in the absorption of the semireduced form of the dyes is observed. Rate constants for triplet quenching (${}^3k_{\text{q}}$) and radical quantum yields (Φ_{R}) are obtained. The results are explained by a very efficient electron-transfer process from PAMAM to xanthene dyes for all of the dye/dendrimer couples that are evaluated.

1. Introduction

Research into dendrimers has attracted much interest due to their unique properties, such as nanoscale size;^[1] the presence of internal cavities in which both ions and neutral molecules can be hosted;^[2] and their capacity for functionalization, which supports the attachment of a high concentration of functional groups on the surface, that aid in their multiple application fields.^[3] A particular class of dendrimers are polyamidoamine (PAMAM) dendrimers, which are commercially available and originate from an ethylenediamine core repetitively branched with amide/tertiary amine subunits (stated as generations, G_x), and ending in a high peripheral density of primary amine functionality (complete generations) or carboxylate groups (half-generations).


Due to the sphere-like shapes of the highest generations, high degree of uniform functionalization, water solubility, and high structural flexibility, PAMAM dendrimers are promising in nanomedicine, biochemistry, and nanotechnology areas.^[4] In spite of the progressive study of biomedical applications, the question regarding the biocompatibility of PAMAM dendrimers still remains. It has been shown that amino-terminated PAMAM becomes toxic at physiological pH because the amino groups are protonated and such emerging cations can disrupt the cellular membranes.^[5] However, several strategies have been adopted to minimize the toxicity of PAMAM dendrimers.^[4b,5b,6]

As a general trend, the study of interactions among dendrimers and dyes or fluorescent probes is relevant to interpret several processes, such as binding, host/guest complexation, and electron or energy transfer.^[7] Kline et al. observed the formation of host/guest complexes between several dyes and PAMAM dendrimers.^[8] Other authors have also reported the selective uptake of dyes into dendrimers.^[2] However, caution needs to be taken when using dye/dendrimer mixtures to determine cellular uptake and fluorescence lifetimes, due to the stochastic nature of the dye/dendrimer biodistribution.^[9]

One attractive application of peripherally functionalized dendrimers is as efficient light-harvesters, because the number of terminal chromophores can be doubled with each generation. Dansylated poly(propyleneimine) (PPI) or poly(propylene amine) (POPAM) dendrimers are known to form occlusion complexes with xanthene dyes.^[2a] The emission spectrum of the dansyl chromophore has a large overlap with the absorption spectrum of xanthene dyes, which enables efficient energy transfer from host to the guest.^[7a,10] Because dansyl absorbs in the UV spectral region and xanthene dyes fluoresce in the visible, such host/guest complexes might be used as tunable light converters through the appropriate selection of guest dye.

Furthermore, the dye/dendrimer couples might find a relevant application in the vinyl polymerization field, as visible-light photoinitiating systems. This is feasible because the amino groups of PAMAM could act as electron donors to excited states of the dyes, leading to radical species capable of initiating polymerization. For this purpose, for over a decade our group has been studying the photophysics and -chemistry of dyes and their interactions with electron donors or acceptors in both homogeneous and microheterogeneous media.^[11] Previously, we characterized the excited states of the dye Safranine O in the presence of PAMAM and PPI dendrimers of low

[a] Dr. E. M. Arbeloa, Dr. C. M. Previtali, Dr. S. G. Bertolotti
Grupo de Fotoquímica
Departamento de Química
Universidad Nacional de Río Cuarto
Consejo Nacional de Investigaciones Científicas y Técnicas (CONICET)
5800 Río Cuarto, Córdoba (Argentina)
E-mail: earbeloa@exa.unrc.edu.ar

 The ORCID identification number(s) for the author(s) of this article can be found under <https://doi.org/10.1002/cphc.201701295>.

generations.^[12] We concluded that dye/dendrimer associations did not occur, and quenching experiments demonstrated that, in this particular case, the amine dendrimers simply acted as electron donors.

More recently, we studied the interactions between the xantheno dye Eosin Y (Eos) and low generations of PAMAM dendrimers in alkaline aqueous solution.^[13] The observed spectral changes were ascribed to dye/dendrimer association and the corresponding binding constants correlated with the size of the dendrimer. These results, along with those from anisotropy and time-resolved fluorescence experiments, suggested partial encapsulation of the dye in the quasi-globular molecule of PAMAM-G3. In a later photochemical study on this system, we performed stationary and laser flash photolysis (LFP) experiments.^[14] Changes in the absorption spectra of the dye after irradiation in the presence of dendrimers were ascribed to the formation of several transient species, which could be ascribed to semireduced and partially debrominated forms of the dye. We inferred a quenching mechanism based on electron transfer from PAMAM to the triplet state of Eos, and the corresponding triplet quenching rate constants and radical quantum yields were determined. From these data, we concluded that the Eos/PAMAM couple might be a promising photoinitiator of vinyl polymerization with low ecological impact.

Herein, we expand our previous work on dye/dendrimer interactions, by studying comparatively the photophysical and -chemical properties of the xantheno dyes Eos, Erythrosin B (Ery), and Rose Bengal (RB) in the presence of amino-terminated PAMAM dendrimers of relatively higher generations (G3–G5), in alkaline aqueous solution (Scheme 1). The absorption

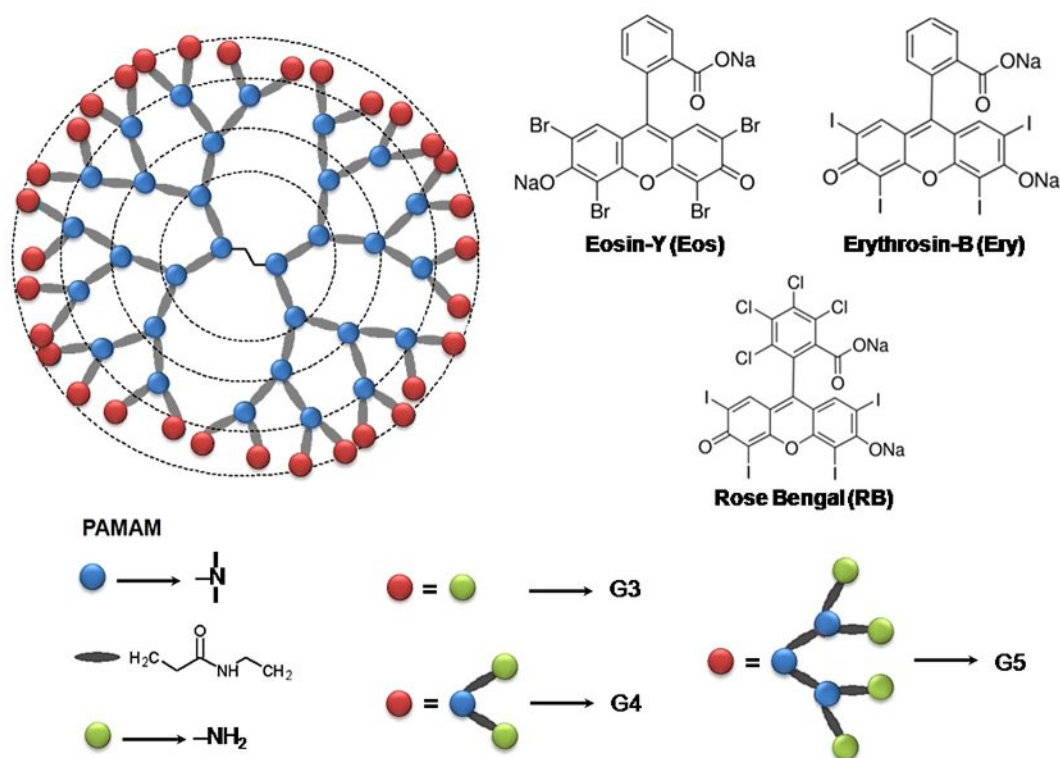
and fluorescence spectra showed bathochromic shifts, which correlated with the size of the dendrimer. The dye/dendrimer binding constants (K_{bind}) were calculated; these indicated strong interactions between both molecules. The rate constants for the triplet-state quenching (3k_q) and radical quantum yields (Φ_R) were also obtained.

2. Results and Discussion

2.1. Absorption and Fluorescence

The absorption and fluorescence spectra of Eos, Ery, and RB in buffered aqueous solutions at pH 10 showed the typical bands of xantheno dyes, the maximum wavelengths of which agreed with reported data.^[15] In the presence of G3, G4, and G5 generations of PAMAM dendrimers, marked redshifts were recorded in both types of spectra for all dyes. At pH 10, the dyes are in their unprotonated dianionic form because all have pK_a values of around 4–6.^[16] Due to the presence of a large number of primary and tertiary amino groups in the structure of PAMAM dendrimers, proper control of the pH is necessary. At pH 10, all amino groups are fully unprotonated, and thus, all dendrimers are uncharged.^[17]

Figure 1 (top) shows the effect of generations G3–G5 on the absorption spectra of the analyzed xantheno dyes, at the same molar concentrations of all dendrimers. As an example, in Figure 1 (bottom) the fluorescence emission of the dyes is compared in the absence and presence of G5 at the same dendrimer concentration as that used to record the absorption



Scheme 1. Structures of the xantheno dyes and amino-terminated PAMAM dendrimers.

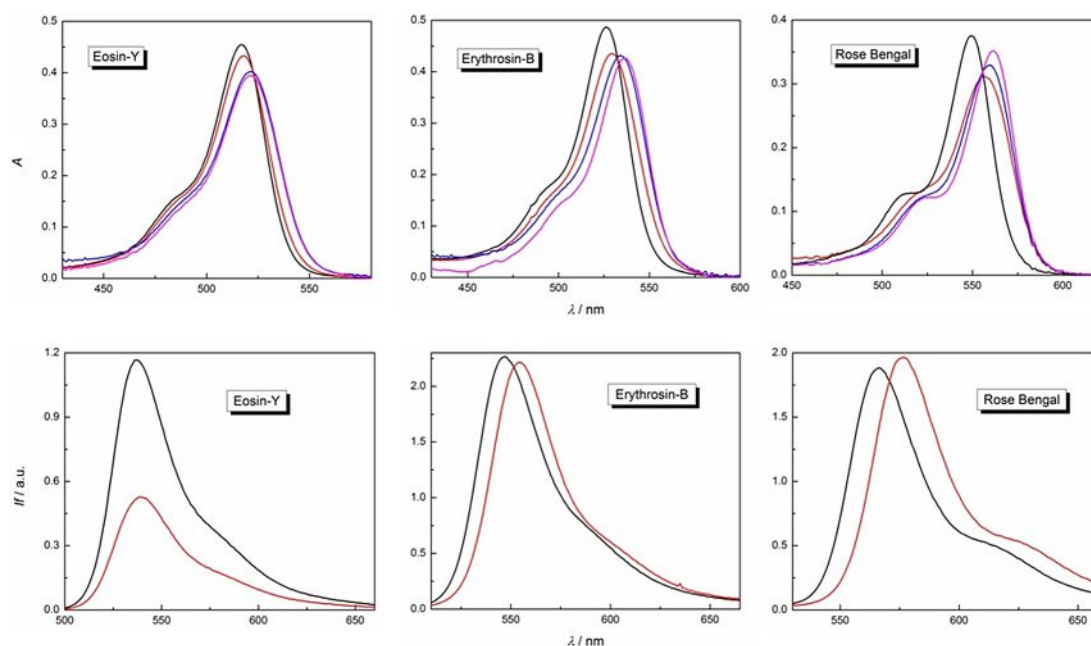


Figure 1. Top: Absorption spectra of xanthene dyes in the absence of PAMAM (black), and in the presence of G3 (red), G4 (blue), and G5 (pink). The concentrations of the dyes and dendrimers were 5 and 40 $\mu\text{mol L}^{-1}$, respectively. Bottom: Fluorescence spectra of the xanthene dyes in the absence (black) and presence (red) of G5 (40 $\mu\text{mol L}^{-1}$).

spectra. Table 1 provides a summary of the results from absorption and emission measurements.

The redshifts in Table 1 may be explained based on the micropolarity of the environment sensed by the dyes in the presence of dendrimers. It is known that in solvents of lower polarity than that of water xanthene dyes experience bathochromic shifts in their absorption and emission bands.^[15a,18] Similar effects have been reported by associating these dyes with different macromolecules. For example, Ery and RB showed redshifts in the presence of aqueous micelles of the surfactants cetyltrimethylammonium bromide (CTAB) and Triton X-100,^[19] the polarities of which are similar to those of *n*-alcohols.^[20] Bathochromic shifts in absorption and fluorescence spectra of Eos bonded to the interface of reverse micelles were also recorded by our group.^[11e] Analogous results were found for xanthene dyes bonded to the proteins lysozyme and bovine serum albumin.^[15b] In particular, the spectral changes recorded for RB (Figure 1) resemble those reported by Lissi et al., concerning RB bonded to human serum albumin (HSA) in aqueous solution.^[21] It is further known that the internal cavities of PPI and PAMAM dendrimers are significantly less polar than that of water.^[22] Several studies on xanthene dyes hosted in non-

water-soluble PPI dendrimers have shown subsequent bathochromic shifts in the absorption and emission spectra.^[2a,7a] In our previous work, we demonstrated that the formation of Eos/PAMAM complexes were characterized by bathochromic shifts that correlated with the size of the dendrimer.^[13] We were able to conclude that Eos sensed a microenvironment of polarity similar to that of 1-propanol, upon interaction with dendrimers. Therefore, our results in Table 1 are in agreement with aforementioned reports and may be ascribed to the formation of the respective dye/dendrimer complexes.

A close examination of the results in Table 1 allows us to infer that there are differences in the magnitude of the interactions between all dye/dendrimer pairs studied. The redshifts ($\Delta\lambda$) in absorption for Eos were 1 and 4 nm upon going from G3 to G5, whereas those for Ery and RB ranged between 4–10 and 8–13 nm, respectively. It can be concluded that, for a given dye, a higher dendrimer size (generation) results in a larger bathochromic shift at comparable PAMAM concentrations. Absorption and fluorescence data in Table 1 also show that $\Delta\lambda$ increases in the order Eos < Ery < RB, for a given generation of PAMAM. It is noteworthy that the higher $\Delta\lambda$ recorded for Eos (in the presence of G4 or G5) is less than the lower $\Delta\lambda$ recorded for RB (in the presence of G3). All of these results suggest that dye/dendrimer association depends not only on the dendrimer size, but also on dye structure.

Fluorescence spectra (Figure 1) also provide evidence of very different interactions between dendrimers and dyes. For example, in the presence of G5, the emission of Eos is notably quenched and a slight redshift of 2 nm is observed, whereas RB shows an increase in the fluorescence intensity and the maximum wavelength is redshifted by 11 nm. Ery shows similar behavior (but not identical) to that of RB. It was previously re-

Table 1. Absorption and fluorescence maxima wavelengths ($\lambda_{\text{max}}^{\text{A}}$ and $\lambda_{\text{max}}^{\text{F}}$, respectively), for xanthene dyes in the absence (water, pH 10) and presence of PAMAM dendrimers (40 $\mu\text{mol L}^{-1}$).

Dye	$\lambda_{\text{max}}^{\text{A}}$ [nm]				$\lambda_{\text{max}}^{\text{F}}$ [nm]	
	Water	G3	G4	G5	Water	G5
Eos	517	518	521	521	537	539
Ery	526	530	534	536	547	555
RB	549	557	560	562	566	577

ported that Eos showed residual fluorescence upon association with dendrimers, although efficient quenching occurred.^[13] Ery and RB also showed fluorescence quenching at dye/dendrimer ratios of > 1 (not shown). Therefore, the increase in fluorescence of Ery and RB observed in Figure 1 can be ascribed to residual emission promoted by strong association with the dendrimer, according to which these dyes sense a less polar environment than that of Eos (as evidenced by larger red-shifts).

To quantify the dye/dendrimer interactions, the absorption data collected were analyzed based on an equilibrium model [Eq. (1)]^[23] to yield the corresponding binding constants [K_{bind} ; Eqs. (2) and (3)]:



$$K_{\text{bind}} = \frac{[\text{Complex}]}{[\text{Dye}_f][\text{PAMAM}_f]} \quad (2)$$

$$\frac{1}{\Delta A} = \frac{1}{[\text{Dye}]K_{\text{bind}}\Delta\epsilon[\text{PAMAM}]} + \frac{1}{[\text{Dye}]\Delta\epsilon} \quad (3)$$

in which the reagents in parentheses refer to their molar concentrations and the subscript f stands for free molecules in solution. In Equation (3), ΔA stands for the absorbance change promoted by the dendrimer at a given wavelength and $\Delta\epsilon$ is the difference in molar extinction coefficients between associated and free dyes. In the present case, the binding constants were determined at the maximum wavelength of the difference (not shown) absorption spectra with and without PAMAM. As an example, in Figure 2, the double reciprocal plots, according to Equation (3), are shown for the dyes in the presence of G5. In all cases, the data fitted well to straight lines and values of K_{bind} were obtained from the respective intercept/slope ratio, as summarized in Table 2.

It should be noted that to obtain K_{bind} , we have assumed a 1:1 complex between dye and dendrimer in all cases. It has been reported that higher dendrimer generations, such as G4 and G5, are able to host more than one dye molecule.^[2a] However, those experiments were performed in organic solvents in which dendrimers are soluble, but xanthene dyes are insoluble. Such experimental conditions prompt the dye to be hosted within the dendrimer. On the other hand, if both dye and den-

Table 2. Binding constants (K_{bind}) for the association between the xanthene dyes Eos, Ery, and RB and PAMAM dendrimers of G3–G5.			
Dye	$K_{\text{bind}} [10^4 \text{ L mol}^{-1}]$		
	G3	G4	G5
Eos	0.80 ± 0.08	4.62 ± 0.07	7.40 ± 0.55
Ery	2.13 ± 0.27	8.37 ± 0.56	36.6 ± 1.4
RB	4.99 ± 0.62	9.30 ± 0.90	41.5 ± 0.1

dimer are water soluble as in the present work, an association equilibrium it is expected. Moreover, at final concentration ratios of about 1:20 (dye/G4) and 1:10 (dye/G5) used herein, the association of more than one dye molecule per dendrimer is extremely improbable.

Several interesting conclusions may be drawn from Table 2. A correlation between K_{bind} values and the size of the dendrimer is observed for the three dyes studied. This trend agrees with our previous report on the association between Eos and low generations (G0–G3) of PAMAM dendrimers in alkaline aqueous solution.^[13] In Table 2, it is also shown that K_{bind} values for dye/G5 complexes were around one order of magnitude greater than those for dye/G3. These differences in K_{bind} values reveal that stronger interactions between the dyes and the bigger dendrimers are occurring, which could lead to the formation of the host/guest complex. Many reports deal with the inclusion of dyes inside both PAMAM and PPI dendrimers.^[2a,8,24] In particular, G4 and G5 are assumed to be globular in solution and their structures have inner void cavities that are capable of accommodating small guest molecules, such as dyes.^[1a,25]

Interestingly, K_{bind} values followed the order Eos/PAMAM < Ery/PAMAM < RB/PAMAM for each PAMAM generation, which suggested a certain selectivity of the dendrimers toward xanthene dyes. This property of dendrimers has already been previously reported by other researchers, with solvatochromic dyes as fluorescent probes.^[2b,26] In the case of xanthene dyes, Balzani et al. demonstrated about a fourfold higher selectivity for RB versus Eos, by means of extraction experiments with peripherally modified PPI-G4 dendrimers in dichloromethane.^[2a] They concluded that the association would be unrelated to dimensions of dye molecules, but strongly dependent on the pH of the initial dye solution and particular (but not elucidated)

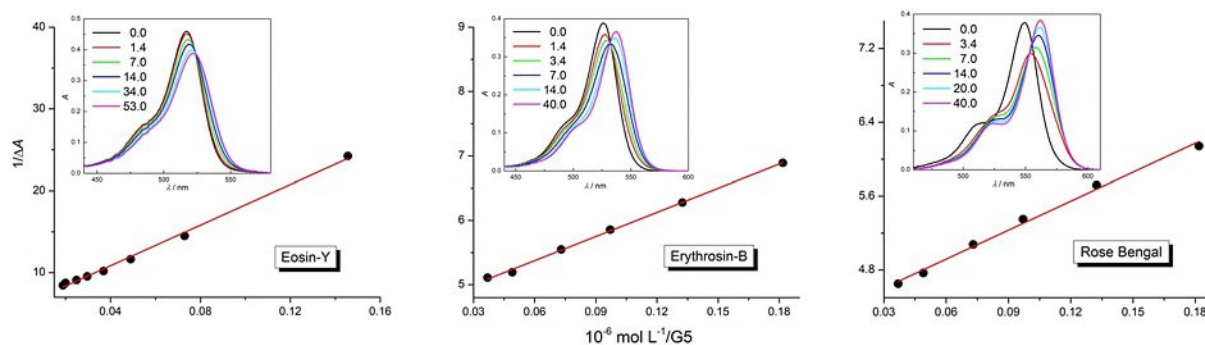


Figure 2. Double reciprocal plots of the absorbance change versus dendrimer molar concentration, according to Equation (3) for xanthene dyes in the presence of G5. Insets show the absorption spectra of each dye in the presence of several G5 concentrations (in $\mu\text{mol L}^{-1}$).

chemical properties. From later computational work, Teobaldi et al. explained this 4:1 selectivity based on aggregation of the dyes because the RB dimer proved to be more favorable than that of the Eos dimer inside the PPI structure.^[27] Although our present data show a similar trend in selectivity (e.g., $K_{\text{bind-RB/G5}} \approx 6K_{\text{bind-Eos/G5}}$), the K_{bind} values were obtained under experimental conditions that excluded the possibility of aggregation of the dyes. Other authors have studied the binding interactions in various supramolecular systems comprised by xanthene dyes and a host (H = enzymes,^[28] micelles,^[29] or polyelectrolytes^[30]), and reported the same sequence of selectivity as that reported herein (i.e., Eos/H < Ery/H < RB/H). They ascribed such results to the hydrophilic–lipophilic balance of the dyes, which depended on the amount and size of halogen atoms in their structure. Based on this criterion, we concluded that RB would be more strongly associated to dendrimers than that of Eos due to more intense hydrophobic interactions.

2.2. Triplet State

The triplet excited state of xanthene dyes has a prominent role in many applications of the dyes, such as photosensitizing and electron-transfer processes.^[16,31] To evaluate the effect of PAMAM dendrimers on the triplet excited state of the dyes, LFP experiments were performed. The transient absorption spectra recorded for Eos, Ery, and RB showed two main difference absorption bands in the $\lambda = 350\text{--}450$ and $550\text{--}700$ nm regions. These absorption bands may be ascribed to the corresponding triplet states of the dyes,^[31a,32] which decayed with lifetimes in the order of $70\text{--}100\ \mu\text{s}$ under the experimental conditions used herein (buffer at pH 10). A shortening of the triplet lifetime was recorded for all dyes in the presence of PAMAM. As an example, in Figure 3, the transient spectra of Ery in the absence and presence of G3 ($25\ \mu\text{mol L}^{-1}$) and G5 ($14\ \mu\text{mol L}^{-1}$) are compared at several time intervals after a laser pulse. At short times, the transient spectra in the presence of PAMAM resemble that of the dye alone, and may be ascribed to the corresponding triplet state. At longer times, only the absorption at $\lambda = 410\text{--}420$ nm remains. It is known that in the absence of quenchers the triplet decay occurs by

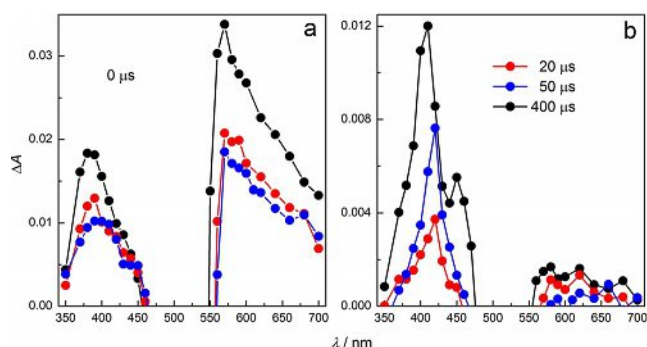


Figure 3. Transient absorption spectra of Ery ($4\ \mu\text{mol L}^{-1}$) in the absence (black), and the presence of G3 ($25\ \mu\text{mol L}^{-1}$; red) and G5 ($14\ \mu\text{mol L}^{-1}$; blue), at short (a) and long (b) times after a laser pulse. Notably, different scaling in the y axis of the two panels is due to the difference in quantum yields and extinction coefficients between triplet and radical species.

self-quenching or triplet–triplet annihilation; these give rise to the respective semireduced and semioxidized transient forms, which absorb at $\lambda \approx 400$ and 450 nm, respectively.^[32] Because PAMAM can act as an electron donor,^[12,14] the band observed at $\lambda = 410\text{--}420$ nm in the presence of dendrimer may be ascribed to the semireduced form of the dye. An alternative mechanism for the photochemical reaction was suggested for a xanthene dye/polyamino sugar system, but we do not think that it applies in the present case.^[33]

The triplet decay of Ery in the presence of PAMAM shows that there is no longer any absorption in the apparent triplet maximum ($\lambda = 570$ nm), from $40\ \mu\text{s}$ onwards (Figure 4). On the other hand, it can be seen that after the triplet decays the radical absorption remains beyond several tens of microseconds. In particular, if the dye is in the presence of G5 (Figure 4b), an initial growth of the absorption at $\lambda = 420$ nm is recorded. This can be explained by assuming a higher molar extinction coefficient of the radical than that of the triplet state at such a wavelength. Similar spectroscopic results were recorded for Eos and RB, but are not shown herein for simplicity.

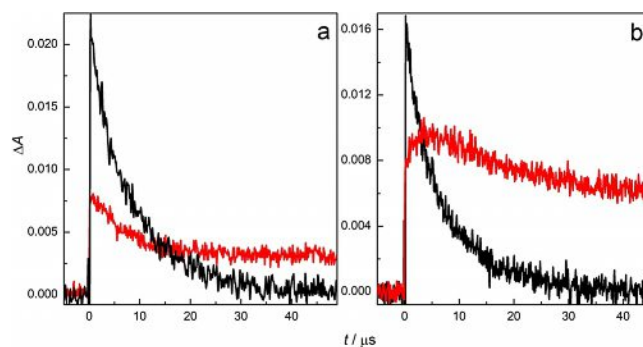


Figure 4. Absorbance time profiles of the triplet state at $\lambda = 570$ nm (black) and the radical species at $\lambda = 420$ nm (red) of Ery ($4\ \mu\text{mol L}^{-1}$) in the presence of a) G3 ($25\ \mu\text{mol L}^{-1}$) and b) G5 ($14\ \mu\text{mol L}^{-1}$).

Quenching of the triplet state of the dyes was observed in the presence of G0 and G3, as recently reported for Eos in alkaline aqueous solution.^[14] The triplet lifetimes (${}^3\tau$) were obtained from the corresponding monoexponential decays at the maximum wavelength of each triplet spectrum. The bimolecular quenching rate constants (3k_q) were evaluated according to Equation (4):

$${}^3\tau^{-1} = \tau_o^{-1} + {}^3k_q[\text{PAMAM}] \quad (4)$$

in which τ_o is the triplet lifetime in the absence of quencher and $[\text{PAMAM}]$ is the dendrimer molar concentration. The Stern–Volmer plots were linear in all cases assessed (Figure 5).

Table 3 provides a summary of the 3k_q values obtained from the slopes of the plots in Figure 5, along with quenching rate constants previously reported by our group for TEOA in aqueous solution.

It can be seen that a similar set of 3k_q values were obtained with each dendrimer and that the data in the presence of G3

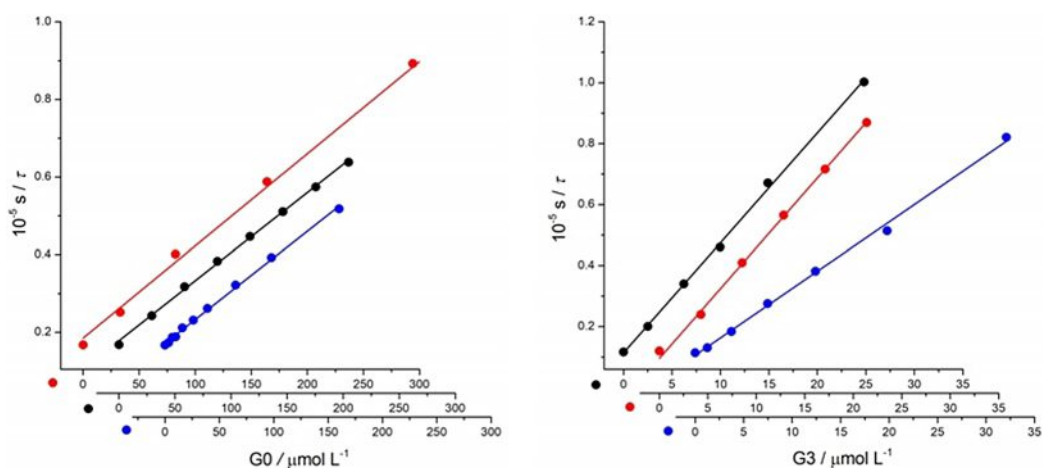


Figure 5. Stern–Volmer plots for the quenching of the triplet excited state of Eos (blue), Ery (black), and RB (red) with G0 and G3 dendrimers in buffer solutions at pH 10. All dye concentrations were $6 \mu\text{mol L}^{-1}$.

Dye	3k_q [$\text{L mol}^{-1} \text{s}^{-1}$]		
	TEOA ^[a]	G0	G3
Eos	4.2×10^7	2.8×10^8	2.5×10^9
Ery	3.8×10^7	2.6×10^8	3.5×10^9
RB	6.4×10^7	2.5×10^8	3.8×10^9

[a] Ref. [27a].

were about one order of magnitude higher than those obtained with G0. A similar correlation between 3k_q and dendrimer size was previously found with Eos by our group, and the data in Table 3 for this dye agree with those reported.^[14] Furthermore, the lowest quenching rate constants obtained herein (with G0) are around one order of magnitude higher than those reported for the aliphatic amine TEOA.

On the other hand, in the presence of G4 and G5, qualitatively analogous decreases in the triplet decay times and ground-state absorbance of the dyes were observed, within the same ranges of dendrimer molar concentrations. As an example, the effect of G5 on both parameters of Ery is shown in Figure 6. According to K_{bind} data in Table 2, a strong association between these globular-shaped dendrimers and the dyes occurs. It is worth noting that the data tend to a plateau at around $14 \mu\text{mol L}^{-1}$ of G5, and at this concentration the dye–dendrimer association increases to about 80%, as estimated from the K_{bind} value. Therefore, the decrease in the triplet mean lifetimes observed in Figure 6 might be ascribed to either the dye sensing a progressive microenvironment polarity change or quenching from amino groups, which is promoted by the formation of the host/guest complex.

A progressive decrease at the zero-time absorption at the maximum of the T–T spectrum (ΔA_T) as a function of dendrimer concentration was also observed for the three dyes. The decays at the maximum wavelengths of the triplet spectra for

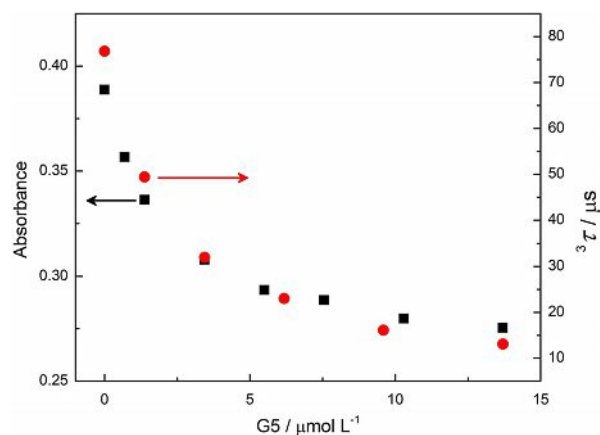


Figure 6. Ground-state absorbance at $\lambda = 526 \text{ nm}$ (■) and triplet decay times (●) of Ery ($4 \mu\text{mol L}^{-1}$) as a function of G5 concentration.

Eos and RB in the presence of increasing amounts of G5 are shown in Figure 7. Figure 7 also compares the effect of G5 concentration on the ground-state absorbance at $\lambda = 532 \text{ nm}$ (the excitation wavelength in LFP experiments) and on the ΔA_T of Eos and RB (see insets in Figure 7, in which both parameters have been denoted as A for simplicity).

As it can be seen, both dyes showed markedly different results. At a concentration of G5 of about $14 \mu\text{mol L}^{-1}$, the ΔA_T value of RB diminishes slightly, whereas in the case of Eos this parameter continues to decrease for G5 concentrations over $30 \mu\text{mol L}^{-1}$. On the other hand, the ground-state absorbance of Eos at $\lambda = 532 \text{ nm}$ increases progressively, whereas it decreases in the case of RB due to binding with G5 (see Section 2.1). The opposite correlation between the absorbed radiation and ΔA_T of Eos, along with significant degradation of the dye after LFP experiments, suggest that the changes in the triplet-state population at zero time are not promoted by dye/dendrimer association, but by a photolysis process. This hypothesis is supported by our previous findings for the photobleaching of Eos in the presence of PAMAM generations G0–

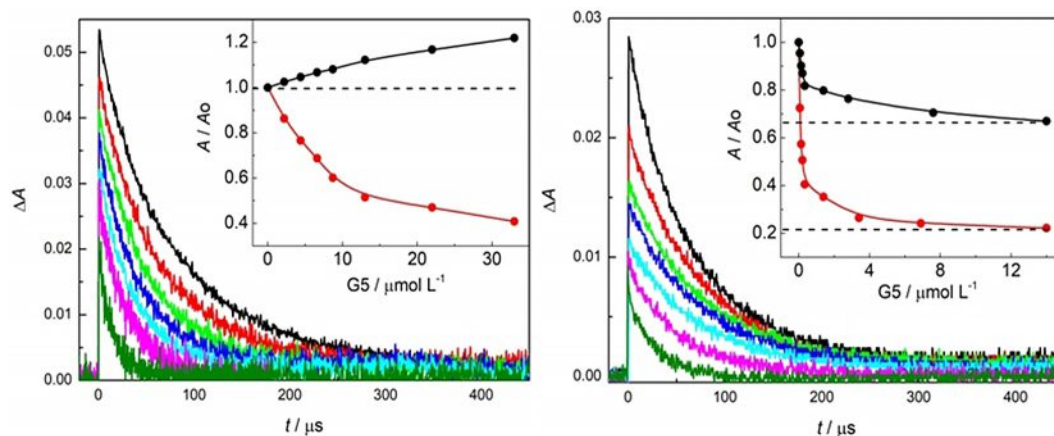


Figure 7. Decays of the triplet state of Eos at $\lambda = 580$ nm (left) and of RB at $\lambda = 590$ nm (right) in the presence of several G5 concentrations. Insets: Absorbance of the ground state at $\lambda = 532$ nm (black) and ΔA_T (red) as a function of the same G5 concentrations as that of the decays. Both parameters were normalized by dividing by the corresponding value in the absence of dendrimer (A_0).

G3.^[14] Figure 7 shows that, in the case of RB, qualitatively analogous descending gradients of both ΔA_T and the ground-state absorption are obtained. Because only slight photolysis of the dye was observed after the laser pulses (less than 5%, data not shown) and this trend resembles that of the triplet decay times depicted on Figure 6, a similar interpretation of the data based on the formation of the host/guest complex can be given here.

To determine the generating efficiencies of the transient species of the dyes, namely, triplet states and radicals, the corresponding quantum yields were evaluated in the presence of PAMAM at concentrations sufficiently high enough to quench the triplet decays times by over 90%. The triplet quantum yields (Φ_T) were determined by means of a relative actinometry, according to Equation (5):

$$(\Phi_T \varepsilon_T)_{\text{Dye}} = \frac{\Delta A_{\text{Dye}}}{\Delta A_{\text{Ref}}} (\Phi_T \varepsilon_T)_{\text{Ref}} \quad (5)$$

in which ΔA is measured at the triplet maximum wavelength of the dyes and a reference, immediately after the laser pulse (extrapolated at zero time), and ε_T is the molar extinction coefficient of the triplet. An alkaline aqueous solution of each xanthene dye in the absence of PAMAM was selected as a reference, the ε_T and Φ_T parameters of which were previously determined by our group.^[31a]

To calculate the Φ_T values from Equation (5), the ground-state depletion method was used to obtain the corresponding ε_T values.^[34] According to this technique, the transient negative difference absorbance at the maximum wavelength of the ground absorption (ΔA_G) was compared with the absorption at the maximum of the T–T spectrum of the dyes (ΔA_T) with the aid of Equation (6):

$$\varepsilon_T = \frac{\Delta A_T}{\Delta A_G} \varepsilon_G \quad (6)$$

In Equation (6), ε_G is the molar extinction coefficient of the ground state at the maximum wavelength of absorbance. Because bleaching in the narrow region near to the ground-state maximum is very similar, but not identical, to the ground-state absorption, the ε_T values determined in this way should be considered as upper-limit values because there could be a small positive contribution of the triplet state to the absorption in the $\lambda = 500$ – 550 nm region.

To assess the radical-generating efficiencies of each dye/dendrimer couple, radical quantum yields (Φ_R) were also estimated by relative actinometry, similarly to Φ_T calculations [see Eq. (5)]. In this case, the absorption remaining after total triplet decay (beyond 100 μs) in the presence of dendrimers measured at $\lambda \approx 410$ – 420 nm (ΔA_R) was used in the left term in Equation (5). The molar extinction coefficient of radical species (ε_R) were determined by the ground-state depletion method, as previously mentioned for ε_T [see Eq. (6)]. Here, ΔA_G was compared with

Table 4. Triplet (Φ_T) and radical (Φ_R) quantum yields of xanthene dyes (Eos, $10 \mu\text{mol L}^{-1}$; Ery, $4 \mu\text{mol L}^{-1}$; and RB, $7 \mu\text{mol L}^{-1}$) in the presence of PAMAM dendrimers (G0, $250 \mu\text{mol L}^{-1}$; G3 $25 \mu\text{mol L}^{-1}$; and G5, $14 \mu\text{mol L}^{-1}$). The corresponding data in water were added for comparison purposes.

Dye		Φ_T	$\Phi_R^{[b]}$
Eos	H ₂ O	0.61 ^[a]	0.25 ^[c]
	G0	0.44	0.17
	G3	0.32	0.09
	G5	0.19	0.08
Ery	H ₂ O	0.97 ^[a]	0.15 ^[c]
	G0	≈ 1	0.08
	G3	0.84	0.11
	G5	0.60	0.14
RB	H ₂ O	0.93 ^[a]	0.15 ^[c]
	G0	0.79	0.07
	G3	0.56	0.06
	G5	0.72	0.12

[a] From Ref. [27a]. [b] Error estimated to be $\pm 10\%$. [c] 20 mmol L^{-1} TEOA (Ref. [27a]).

the absorption at the maximum of the spectrum of the semireduced dye (ΔA_R) with the aid of Equation (6). Table 4 provides a summary of the data obtained, along with Φ_T and Φ_R previously reported for alkaline aqueous solutions of the respective dyes.

Table 4 shows that Φ_T values of the xanthene dyes in the presence of PAMAM were lower than those corresponding to an aqueous solution free from dendrimers. As discussed above, such differences might be explained by either photolysis or association processes. Other authors have estimated a reduction of around 50% in the Φ_T value of RB bound to HSA protein, with respect to its value in solution.^[21] Because lasting photolysis of the dye was not observed, they ascribed such results to other unknown processes from the triplet state, which slowly relax to the ground state. Another possible cause that could contribute to the lowering of Φ_T is a fast singlet excited-state relaxation competing with intersystem crossing, as suggested by Aumanen et al.^[7a,10] These authors were able to detect such fast relaxation from deactivation pathways of xanthene dyes hosted inside of PPI dendrimers, by working on the sub-picosecond timescale. They estimated $\Phi_T \approx 0.6$ – 0.7 for RB hosted in PPI dendrimers ($\approx 30\%$ lower than in water); this agrees with our result.

At a glance, the Φ_R values (Table 4) do not seem to correlate with the magnitude of dye/dendrimer association (Table 2). However, care must be taken upon analyzing the Φ_R values because radicals originate from the triplet states and the efficiencies formation (Φ_T) of these transient species are dependent on the dye/dendrimer couple type. By analyzing both parameters together (i.e., Φ_R/Φ_T ratio), it can be seen that almost twice the conversion of triplet to radical was obtained with Eos (≈ 30 – 40%) relative to those with Ery or RB (≈ 10 – 20%). From K_{bind} data, it can be calculated that, at the dendrimer concentrations used in the LFP experiments, the association extent of Eos ($\approx 40\%$) is about half of that corresponding to Ery and RB ($\approx 80\%$). Because a more strongly associated dye/dendrimer complex would be more difficult to separate into radicals, back recombination would be favored in the case of Ery and RB (so reducing the net formation of radicals). Furthermore, it is interesting to note that the higher Φ_R values obtained herein are similar to those previously reported by our group with TEOA as a quencher, which is proven to be an efficient electron donor.^[31a] Data in Table 4 also show that all Φ_R values were higher than those found for Eos/TEOA in reverse micelles of sodium bis(2-ethylhexyl) sulfosuccinate (AOT; $\Phi_R = 0.006$) and benzylhexadecyldimethylammonium chloride (BHDC; $\Phi_R = 0.024$),^[11e] which have been successfully used as photoinitiating systems of vinyl polymerization to obtain latex nanoparticles.^[31b]

3. Conclusions

We demonstrated how the photophysical properties of xanthene dyes were modified in the presence of G3–G5 PAMAM dendrimers, in buffer solutions at pH 10. From binding analyses, it was concluded that the magnitude of such changes correlated with dendrimer size, and these results agreed with our

previous studies on Eos/PAMAM interactions. We observed certain selectivity in the binding between the dendrimers and the dyes assessed, which was ascribed to the hydrophilic-lipophilic balance of the dyes, and might be interesting and useful to study various applications, such as contaminant extraction, host/guest systems, and drug delivery.

The triplet quantum yields obtained for the dyes in the presence of PAMAM were lower than those in water. The interpretation of these results was complex because Φ_T values were dependent on dendrimer concentration, but photolysis and host/guest complex formation processes were suggested. Also, the radical quantum yields were in the order of, or higher than, those previously reported with typical dye/amine couples in both aqueous and microheterogeneous media. Data showed an inverse correlation between association extent and efficiency of radical formation, which would allow the selection of the appropriate acceptor/donor pair for specific applications. For example, these results suggested that xanthene dye/PAMAM combinations might be used in electron-transfer reactions, such as photoinitiating systems of vinyl polymerization, with low ecological impact; a topic that is currently being explored by our group.

Experimental Section

Xanthene dyes Eos, Ery, and RB and amino-terminated PAMAM dendrimers of several generations in methanol (G0 and G3 20%, G4 10%, and G5 5%) were purchased from Aldrich and used without further purification. Solutions of dendrimers were properly diluted with HPLC-grade methanol (Sintorgan), as necessary. Aqueous solutions were prepared with HPLC-grade water (Sintorgan) and were adjusted to pH 10 with analytical-grade buffer ($\text{HCO}_3^-/\text{OH}^-$).

Absorption spectra were recorded on a Hewlett Packard 6453E diode array spectrophotometer. Emission spectra were measured with a Horiba Jobin Yvon FluoroMax-4 spectrofluorometer. A 1 cm path length quartz cuvette was used in all spectroscopic assays. In absorption measurements, the absorbances were adjusted by about 0.3–0.6 at the respective maximum wavelengths, and about 0.05 at excitation wavelengths for emission experiments. The concentrations of xanthene dyes in the solutions were calculated from the respective molar extinction coefficients (ϵ_i), which were experimentally obtained by absorption spectroscopy, according to the Lambert–Beer law ($\epsilon_{517} = 91100 \text{ L mol}^{-1} \text{ cm}^{-1}$; $\epsilon_{526} = 98000 \text{ L mol}^{-1} \text{ cm}^{-1}$, and $\epsilon_{549} = 101300 \text{ L mol}^{-1} \text{ cm}^{-1}$ for Eos, Ery, and RB, respectively). Throughout all experiments, the addition of dendrimers was performed by using microsyringes under constant stirring, such that the methanol contents in the dyes solutions were $< 5\%$. There were no changes in the spectra attributed to this additional methanol, as verified through blank tests. All data were properly corrected by dilution effects. The measurements were performed at least in duplicate.

Transient absorption spectra and triplet quenching were determined by LFP. A Spectron SL400 Nd:YAG laser generating $\lambda = 532 \text{ nm}$ laser pulses (20 mJ per pulse, ca. 18 ns full-width at half-maximum) was the excitation source. The experiments were performed in a right-angle geometry. The laser beam was defocused to cover the entire path length (10 mm) of the analyzing beam from a 150 W Xe lamp. The detection system comprised a PTI mon-

ochromator coupled to a Hamamatsu R666 PM tube. The signals were acquired and averaged by means of a digital oscilloscope (DSO6012A Agilent Technologies) and then transferred to a computer. All photolysis determinations were performed at $(25 \pm 1)^\circ\text{C}$, and the solutions were deoxygenated by bubbling with solvent-saturated, high-purity argon.

Acknowledgements

This work was supported by the Agencia Nacional de Promoción Científica y Tecnológica (PICT: 1224/2013), CONICET (PIP: 2015-11220150100687CO), and the Universidad Nacional de Río Cuarto.

Keywords: dendrimers · dyes/pigments · photochemistry · photophysics · time-resolved spectroscopy

- [1] a) D. A. Tomalia, A. M. Naylor, W. A. Goddard, *Angew. Chem. Int. Ed. Engl.* **1990**, *29*, 138–175; *Angew. Chem.* **1990**, *102*, 119–157; b) D. A. Tomalia, *Soft Matter* **2010**, *6*, 456–474; c) L. M. Bronstein, Z. B. Shifrina, *Chem. Rev.* **2011**, *111*, 5301–5344.
- [2] a) V. Balzani, P. Ceroni, S. Gesteremann, M. Gorka, C. Kauffmann, F. Vögtle, *Tetrahedron* **2002**, *58*, 629–637; b) E. J. Morgan, J. M. Rippey, S. A. Tucker, *Appl. Spectrosc.* **2006**, *60*, 551–559.
- [3] D. Astruc, E. Boisselier, C. Ornelas, *Chem. Rev.* **2010**, *110*, 1857–1959.
- [4] a) P. Kesharwani, K. Jain, N. K. Jain, *Prog. Polym. Sci.* **2014**, *39*, 268–307; b) N. Taghavi Pourianazar, P. Mutlu, U. Gunduz, *J. Nanopart. Res.* **2014**, *16*, 2342; c) E. R. Figueroa, A. Y. Lin, J. Yan, L. Luo, A. E. Foster, R. A. Drezek, *Biomaterials* **2014**, *35*, 1725–1734; d) Z. Qiao, X. Shi, *Prog. Polym. Sci.* **2015**, *44*, 1–27; e) J. Yang, Q. Zhang, H. Chang, Y. Cheng, *Chem. Rev.* **2015**, *115*, 5274–5300; f) P.-Y. Yang, S.-P. Ju, Y.-C. Chuang, H.-Y. Chen, *Comput. Mater. Sci.* **2017**, *137*, 144–152.
- [5] a) S. P. Mukherjee, F. M. Lyng, A. Garcia, M. Davoren, H. J. Byrne, *Toxicol. Appl. Pharmacol.* **2010**, *248*, 259–268; b) K. Jain, P. Kesharwani, U. Gupta, N. K. Jain, *Int. J. Pharm.* **2010**, *394*, 122–142; c) A. Janaszewska, K. Maczynska, G. Matuszko, D. Appelhans, B. Voit, B. Klajnert, M. Bryszewska, *New J. Chem.* **2012**, *36*, 428–437.
- [6] Y. Cheng, L. Zhao, Y. Li, T. Xu, *Chem. Soc. Rev.* **2011**, *40*, 2673–2703.
- [7] a) J. Aumanen, J. Korppi-Tommola, *Chem. Phys. Lett.* **2011**, *518*, 87–92; b) J. Han, C. Gao, *Curr. Org. Chem.* **2011**, *15*, 2–26; c) C. A. Dougherty, J. C. Furgal, M. A. van Dongen, T. Goodson III, M. M. Banaszak Holl, J. Manono, S. DiMaggio, *Chem. Eur. J.* **2014**, *20*, 4638–4645.
- [8] K. K. Kline, E. J. Morgan, L. K. Norton, S. A. Tucker, *Talanta* **2009**, *78*, 1489–1491.
- [9] C. A. Dougherty, S. Vaidyanathan, B. G. Orr, M. M. Banaszak Holl, *Bioconjugate Chem.* **2015**, *26*, 304–315.
- [10] J. Aumanen, V. Lehtovuori, N. Werner, G. Richardt, J. van Heyst, F. Vögtle, J. Korppi-Tommola, *Chem. Phys. Lett.* **2006**, *433*, 75–79.
- [11] a) G. V. Porcal, C. M. Previtali, S. G. Bertolotti, *Dyes Pigm.* **2009**, *80*, 206–211; b) G. V. Porcal, E. M. Arbeloa, D. E. Orallo, S. G. Bertolotti, C. M. Previtali, *J. Photochem. Photobiol. A* **2011**, *226*, 51–56; c) G. V. Porcal, M. S. Altamirano, S. G. Bertolotti, C. M. Previtali, *J. Photochem. Photobiol. A* **2011**, *219*, 62–66; d) G. V. Porcal, C. A. Chesta, M. A. Biasutti, S. G. Bertolotti, C. M. Previtali, *Photochem. Photobiol. Sci.* **2012**, *11*, 302–308; e) E. M. Arbeloa, G. V. Porcal, S. G. Bertolotti, C. M. Previtali, *J. Photochem. Photobiol. A* **2013**, *252*, 31–36; f) M. S. Altamirano, M. E. Grassano, S. G. Bertolotti, C. M. Previtali, *J. Photochem. Photobiol. A* **2016**, *329*, 149–154; g) G. V. Porcal, E. M. Arbeloa, S. G. Bertolotti, C. M. Previtali, *J. Photochem. Photobiol. A* **2017**, *346*, 187–193.
- [12] C. A. Suchetti, A. I. Novaira, S. G. Bertolotti, C. M. Previtali, *J. Photochem. Photobiol. A* **2009**, *201*, 69–74.
- [13] E. M. Arbeloa, C. M. Previtali, S. G. Bertolotti, *J. Lumin.* **2016**, *172*, 92–98.
- [14] E. M. Arbeloa, C. M. Previtali, S. G. Bertolotti, *J. Lumin.* **2016**, *180*, 369–375.
- [15] a) G. R. Fleming, A. W. E. Knight, J. M. Morris, R. J. S. Morrison, G. W. Robinson, *J. Am. Chem. Soc.* **1977**, *99*, 4306–4311; b) Y. Zhang, H. Görner, *Photochem. Photobiol.* **2009**, *85*, 677–685.
- [16] D. C. Neckers, O. M. Valdes-Aguilera in *Advances in Photochemistry*, Wiley, Hoboken, **2007**, pp. 315–394.
- [17] a) D. Cakara, J. Kleimann, M. Borkovec, *Macromolecules* **2003**, *36*, 4201–4207; b) P. K. Maiti, T. Çagin, S.-T. Lin, W. A. Goddard, *Macromolecules* **2005**, *38*, 979–991.
- [18] a) M. A. Rauf, J. P. Graham, S. B. Bukallah, M. A. S. Al-Saedi, *Spectrochim. Acta Part A* **2009**, *72*, 133–137; b) M. Chakraborty, A. K. Panda, *Spectrochim. Acta Part A* **2011**, *81*, 458–465.
- [19] B. B. Bhowmik, P. Ganguly, *Spectrochim. Acta Part A* **2005**, *61*, 1997–2003.
- [20] K. A. Zachariasse, P. Nguyen Van, B. Kozankiewicz, *J. Phys. Chem.* **1981**, *85*, 2676–2683.
- [21] E. Alarcon, A. M. Edwards, A. Aspee, C. D. Borsarelli, E. A. Lissi, *Photochem. Photobiol. Sci.* **2009**, *8*, 933–943.
- [22] a) G. Pistolis, A. Malliaris, C. M. Paleos, D. Tsiourvas, *Langmuir* **1997**, *13*, 5870–5875; b) D. L. Richter-Egger, J. C. Landry, A. Tesfai, S. A. Tucker, *J. Phys. Chem. A* **2001**, *105*, 6826–6833; c) G. Pistolis, A. Malliaris, *Langmuir* **2002**, *18*, 246–251.
- [23] H. A. Benesi, J. H. Hildebrand, *J. Am. Chem. Soc.* **1949**, *71*, 2703–2707.
- [24] D. L. Richter-Egger, A. Tesfai, S. A. Tucker, *Anal. Chem.* **2001**, *73*, 5743–5751.
- [25] T. Li, K. Hong, L. Porcar, R. Verduzco, P. D. Butler, G. S. Smith, Y. Liu, W.-R. Chen, *Macromolecules* **2008**, *41*, 8916–8920.
- [26] K. K. Kline, S. A. Tucker, *J. Phys. Chem. A* **2010**, *114*, 7338–7344.
- [27] G. Teobaldi, M. Melle-Franco, F. Zerbetto, *J. Chem. Theory Comput.* **2005**, *1*, 194–200.
- [28] T. N. Kirillova, M. A. Gerasimova, E. V. Nemtseva, N. S. Kudryasheva, *Anal. Bioanal. Chem.* **2011**, *400*, 343–351.
- [29] D. S. Pellosi, B. M. Estevão, J. Semensato, D. Severino, M. S. Baptista, M. J. Politi, N. Hioka, W. Caetano, *J. Photochem. Photobiol. A* **2012**, *247*, 8–15.
- [30] E. Slyusareva, M. Gerasimova, V. Slabko, N. Abuzova, A. Plotnikov, A. Eychmüller, *Chemphyschem* **2015**, *16*, 3997–4003.
- [31] a) M. V. Encinas, A. M. Rufs, S. G. Bertolotti, C. M. Previtali, *Polym.* **2009**, *50*, 2762–2767; b) E. Arbeloa, G. Porcal, S. Bertolotti, C. Previtali, *Colloid Polym. Sci.* **2015**, *293*, 625–632.
- [32] A. Seret, A. Van de Vorst, *J. Phys. Chem.* **1990**, *94*, 5293–5299.
- [33] E. A. Slyusareva, A. G. Sizykh, M. A. Gerasimova, V. V. Slabko, S. A. Myslivets, *Quantum Electron.* **2012**, *42*, 687.
- [34] R. Bonneau, I. Carmichael, G. L. Hug *Pure Appl. Chem.* **1991**, *63*, 289–299.

Manuscript received: November 30, 2017
Accepted manuscript online: January 8, 2018
Version of record online: February 19, 2018